

COUPLING MULTI-BODY AND FLUID DYNAMICS ANALYSIS WITH PRECICE AND MBDYN

CLAUDIO G. CACCIA* AND PIERANGELO MASARATI†

*Department of Aerospace Science and Technology, Politecnico di Milano
via La Masa 34, 20156, Milan, Italy
e-mail: claudiogiovanni.caccia@mail.polimi.it, web page: <http://www.aero.polimi.it/>

†Department of Aerospace Science and Technology, Politecnico di Milano
via La Masa 34, 20156, Milan, Italy
e-mail: pierangelo.masarati@polimi.it, web page: <http://www.aero.polimi.it/>

Key words: Multibody System Dynamics, Cosimulation, Fluid-Structure Interaction

Abstract.

The software library preCICE allows to connect single physics solvers to perform multiphysics cosimulations in a partitioned way. We interfaced preCICE with the multibody dynamics software MBDyn and assessed its performance with the set of well-known benchmarks proposed by Turek and Hron. The set-up consists of a laminar incompressible flow around a slender elastic object, which is suitable to be simulated via MBDyn beam elements connected to a cloud of interface points.

1 MOTIVATION

In this work, the Multibody Dynamics solver MBDyn¹ [10] has been interfaced with the multiphysics coupling library preCICE [3] to extend MBDyn capabilities to solve fluid structure interaction (FSI) problems.

MBDyn is a free general-purpose Multibody Dynamics solver developed at the Department of Aerospace Science and Technology of Politecnico di Milano, which models the constrained nonlinear dynamics of rigid and flexible bodies formulated as sets of Differential-Algebraic Equations (DAEs) [10].

When FSI simulations involve slender and flexible structures, it is particularly interesting to use a reduced dimensionality finite element model (i.e. a set of *beams* or *shells*) along with a form of mapping between the interface (wet surface) and the structural model, especially when the two are topologically incompatible, in order to exchange the mutual kinematics and dynamics [12].

¹<https://www.mbdyn.org/>, last accessed May 2021.

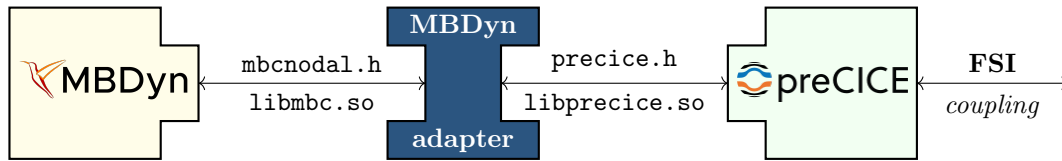


Figure 1: MBDyn adapter interface scheme

MBDyn models slender deformable components using an original, geometrically exact finite volume formulation for beam elements with a high level of flexibility [8, 1]. MBDyn is also able to exchange kinematics and load information with a cloud of external points of arbitrary topology [12].

PreCICE is an increasingly popular open-source coupling library which provides the components to connect traditional single-physics solvers to generate a partitioned multi-physics simulation (e.g. fluid-structure interaction, conjugated heat transfer, solid-solid interaction, etc.).

The implementation of an *adapter* connecting MBDyn and preCICE represents an advantage and an extension of capabilities for both applications. On the one hand, various preCICE adapters for fluid solvers have already been developed. MBDyn can connect in a standardized way to a considerable number of codes, including many popular, well-validated open source and commercial ones [18]², thus extending its aeroservoelasticity simulation capabilities (e.g. [4]).

On the other hand, with a fully integrated MBDyn adapter, the library preCICE gains the opportunity to connect to a multibody dynamics software, which has not yet been completely developed and tested in many contexts and applications.

2 ADAPTER DESCRIPTION

An *adapter* is the “glue-code” that allows the interface of an existing software component to be used by another component without modifying its source code. In the present case it is possible to exploit the APIs given by MBDyn and preCICE, so that the adapter itself is independent from both codes (see Fig. 1).

2.1 MBDyn Features

MBDyn can simulate linear and non-linear dynamics of rigid and flexible bodies (including geometrically exact and composite-ready beam and shell finite elements, component mode synthesis elements, lumped elements) subjected to kinematic constraints, external forces and control subsystems [10]. *Nodes* are the basic blocks of an MBDyn model: they instantiate kinematic degrees of freedom and the corresponding equilibrium equations. *Elements* constitute the components of the multi-body model. With minor exceptions, each of them connects one or more nodes. They write contributions to equations instanti-

²for an updated list see <https://precice.org/adapters-overview.html>

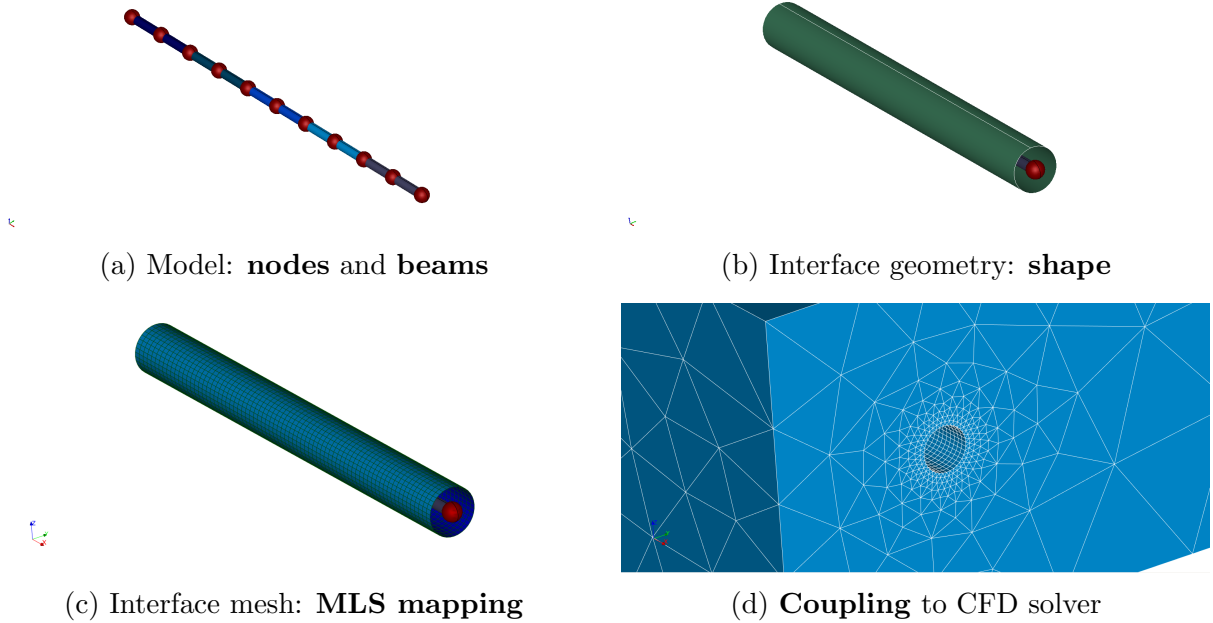


Figure 2: steps to perform FSI with MBDyn

ated by nodes and thus represent the *connectivity* and *constitutive properties* of a model. The *beam* element is defined by its nodes, a reference line (Fig. 2a), and the orientation of the beam *section*. The Finite Volume approach described in [8] is used to model the beam element. The user defines a section constitutive law that is independent from the shape of the beam itself (Fig. 2b), thus the aerodynamic aspects and the structural aspects are handled by two distinct elements of the model.

In MBDyn, it is possible to exchange kinematic and dynamic information and to steer the multi-body simulation from an external software (left side of Fig. 1). This information can be exchanged directly on the nodes or on a cloud of external points, used for example to define an interface geometry in FSI problems (e.g. the mesh in Fig. 2c). The mapping consists in a constant matrix that computes the movement of the external points as functions of those of the nodes, based on the *Moving Least Squares* (MLS) technique [12]. This feature takes care of the topological inconsistency between the nodes and the interface, thus simplifying the mapping at the wet surface, as the interface mesh can be the same on both sides (Fig. 2d).

2.2 preCICE Features

The Open Source library preCICE aims at coupling existing solvers in a partitioned black-box manner [6]: only minimal information about each solver is required; the connection only involves the interface nodes.

In a nutshell, preCICE simply affects the input and observes the output of the solvers

(called *participants*). The required data and control elements are accessed using an *adapter* (right side of Fig. 1).

The actions required to perform a coupled simulation involve: the set up of the communication between the participants, the computation of the mapping of data between meshes, the implementation of the coupling strategy, the verification of convergence, and the steering of the simulation.

2.3 Adapter Configuration

The *adapter* has been implemented in C++ and is currently available from GitLab³.

The code is conceptually divided in two classes. The main class implements the functions given by the preCICE interface and has access to the other class, which takes care of all the aspects regarding MBDyn.

Some data are needed in order to perform a simulation. Such data are stored in a JSON file given as input. This information concerns:

- *setup*: communication with preCICE and MBDyn, mesh location for coupling and mapping
- *run*: type of data to pass, parameters to progressively load the structure at the beginning of simulation
- *output*: forces, displacements and velocities at interface nodes (Fig. 3), resultant force and resultant moment.

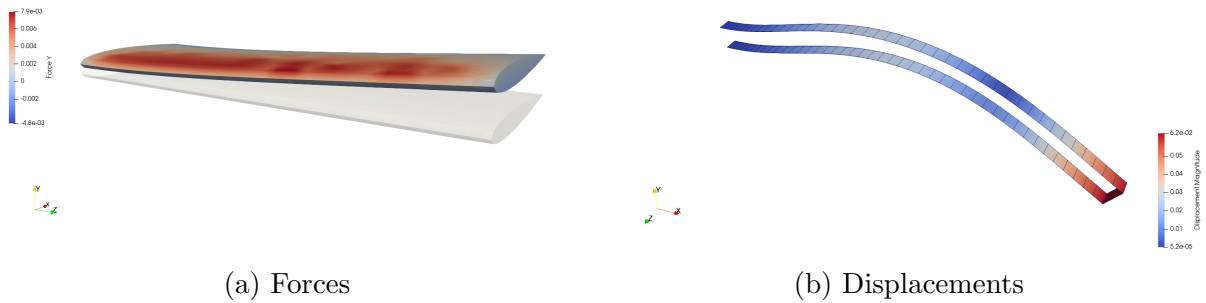


Figure 3: Simulation output

³<https://public.gitlab.polimi.it/DAER/mbdyn/-/wikis/preCICE-MBDyn-adapter>

3 VALIDATION OF THE COMPONENTS

In order to validate the coupling adapter developed, we simulated some test cases to confirm the correctness of the implementation.

The three Turek-Hron FSI test cases described in [14] are a set of well-known benchmarks in FSI literature. They are characterized by the same domain (a circular cylinder with a trailing flap) and the same fluid properties. Differences are only related to fluid velocity and structural properties (in particular the density, ρ , and Young's modulus, E).

Besides, they are all characterized by a high *mass ratio* $M = \frac{\rho_F}{\rho_S}$ between the fluid and structural density, which is known to lead to algorithmic instability of the coupled system (e.g. [7, 11]).

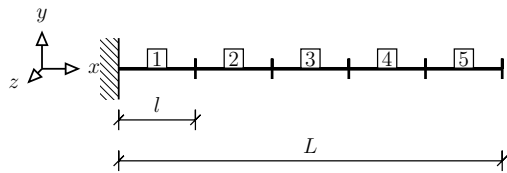
All the presented results are compared to the “reference” data (i.e. defined as almost grid-independent in [14]) obtained using a fully implicit monolithic ALE-FEM method with a fully coupled multigrid solver.

3.1 Validation of the Structural Part

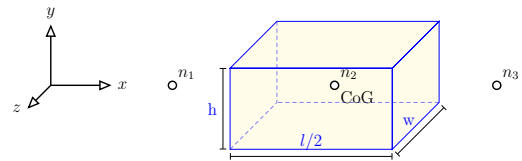
The tests named CSM in [14] are used to fit the structural part. The beam is loaded only with gravitational force $\vec{g} = (0, g) = 2 \text{ m s}^{-2}$. Tests CSM1 and CSM2 are steady state solutions at different Young's modulus, while CSM3 is a time dependent solution starting from the undeformed configuration.

An MBDyn cantilever beam model composed of three-node `beam3` elements [8] has been developed, as depicted in Fig. 4a. The beam section is uniform and rectangular ($w \times h$); the geometrical and physical properties (ρ , E , ν) are constant throughout the length of the beam.

The inertia of the structure is provided by 2 `rigid body` elements attached to the second and third node of each beam element. The center of gravity of each body is placed at the corresponding node (see Fig. 4b). Special bodies are used for the first and last element, with the correct mass, inertia moments, and center of mass location.



(a) Cantilever made of 5 `beam` elements



(b) Body attached to node 2 of the `beam`

The main parameter considered in the analysis is the number of beam elements: tests with 4 or 5 elements give results closest to the benchmark (see Table 1), while a higher number of elements makes the structure more flexible.

Table 1: Comparison of tip displacement (in mm)

# el.	CSM1		CSM2		CSM3		
	u_x	u_y	u_x	u_y	u_x	u_y	f [Hz]
4	-7.28	-66.69	-0.47	-17.13	-14.46 ± 14.46	-65.10 ± 65.82	1.125
5	-7.73	-68.68	-0.51	-17.67	-15.29 ± 15.29	-66.69 ± 68.11	1.104
10	-8.74	-72.90	-0.58	-18.83	-17.57 ± 17.57	-70.82 ± 71.20	1.062
ref.	-7.19	-66.10	-0.47	-16.97	-14.31 ± 14.31	-63.61 ± 65.16	1.099

3.2 Validation of the Fluid Part

The fluid part has been modeled with OpenFOAM, using a hexahedral mesh with different levels of refinement (Fig. 5).

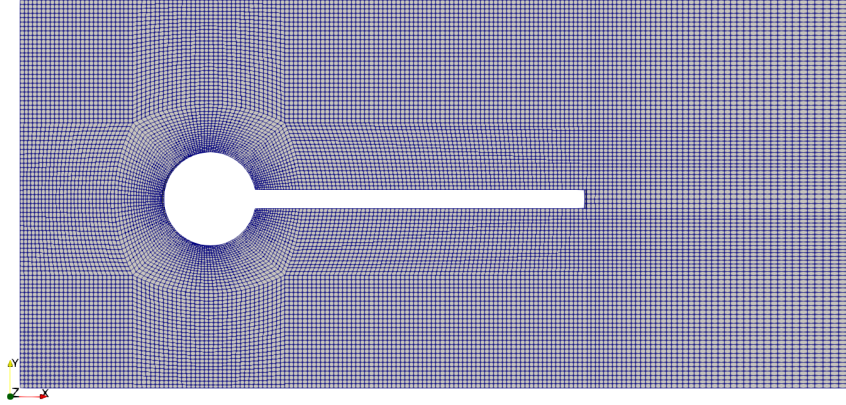


Figure 5: Fluid mesh used for CFD and FSI simulations

The tests named CFD in [14] have been used to understand the fitness of the fluid part. All 3 cases share the same fluid properties, a parabolic inlet profile and a rigid domain. They differ only in average fluid velocity, with values of 0.2, 1 and 2 m s^{-1} . The results are shown in Table 2: at low fluid speed the impact of the fineness of the mesh is low or negligible, whereas it becomes relevant for CFD3, characterized by alternating vortices developing downstream of the structure.

Table 2: Comparison of lift and drag (in N m^{-1})

size	CFD1		CFD2		CFD3		
	drag	lift	drag	lift	drag	lift	f [Hz]
25k	14.28	1.11	139.49	10.77	442.53 ± 4.75	-17.39 ± 384.22	4.38
49k	14.28	1.11	137.34	10.46	441.45 ± 5.17	-15.51 ± 412.03	4.41
ref.	14.29	1.12	136.7	10.53	439.45 ± 5.62	-11.89 ± 437.81	4.3956

4 TEST CASES

Once the solid and the fluid models have been assessed, we considered the FSI test cases described in [14].

4.1 General Set-Up

For each simulation we used the staggered implicit coupling algorithm implemented in preCICE, with the structural component as the first participant and the fluid component as the second one. We considered the IQN-ILS algorithm ([2, 5]) and a filter in order to drop nearly dependent columns [9]. The convergence criteria have been set to a relative error of 10^{-4} for both displacements and forces. This execution order proved to converge much faster than the reciprocal, as interface displacements converge much faster than the forces, which thus benefit of the acceleration algorithm. A parallel implicit coupling [11] has yet to be assessed. All the simulations considered here use a $\Delta t = 1$ ms.

4.2 FSI1

The first test case is characterized by a *mass ratio* $M = 1$ and an average *Reynolds number* $Re = 20$. The position of the beam is not symmetric such that the lift is not zero [17]. The final solution is steady (see Figure 6). It is nevertheless interesting because its high mass ratio and low fluid velocity make the interaction stronger and the convergence sometimes more difficult in partitioned algorithms. The results, in terms of tip displacement and forces on the structure, are shown in Table 3 and compared with the reference in [14].

The coupled simulation converged with an average number of 2.8 iterations. There is no significant difference with respect to the mesh size, and the results are close to the reference.

4.3 FSI2

The second test case is characterized by a *mass ratio* $M = 0.1$ and an average *Reynolds number* $Re = 100$. This test case is fully oscillating while the same problem, considering the structure rigid (CFD2 in [14]) is steady: for this reason, it is considered an excellent

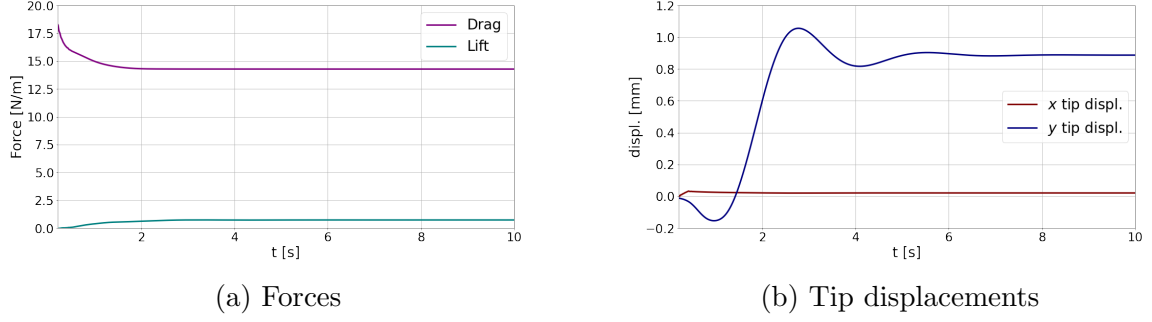


Figure 6: FSI1 Simulation: 5 beams - 49k cells

Table 3: FSI1 results

size	u_x [mm]	u_y [mm]	drag [N m^{-1}]	lift [N m^{-1}]
25k	0.021	0.884	14.279	0.732
49k	0.021	0.887	14.283	0.733
ref.	0.023	0.821	14.295	0.764

check for interaction mechanisms [15]. Besides, it produces the largest deformation and in some cases it is considered the most difficult of the three benchmarks [13].

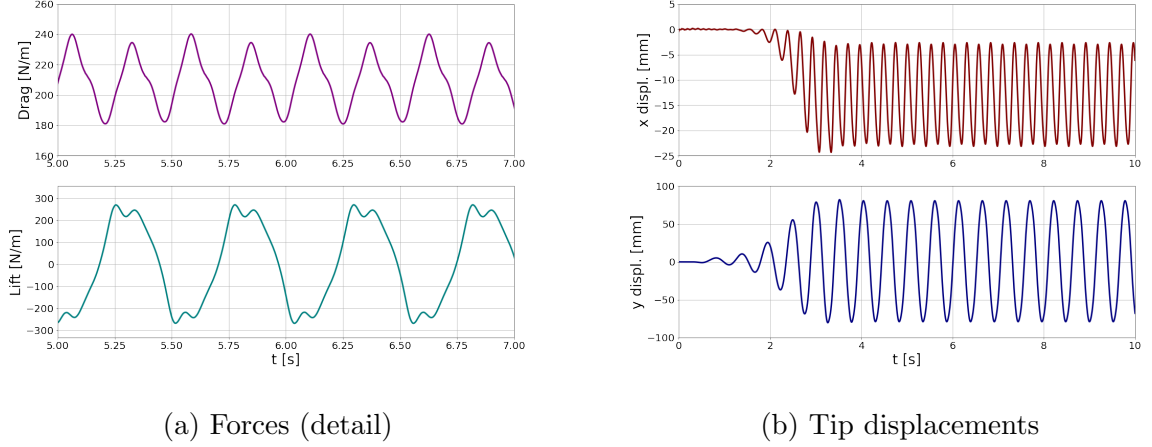


Figure 7: FSI2 Simulation: 5 beams - 49k cells

The behavior of the structure in terms of tip displacement (mean value, amplitude and frequency) is shown in Table 4, while drag and lift on the whole structure are shown in

Table 5.

Table 4: FSI2 results (displacements)

size	u_x [mm]	f [Hz]	u_y [mm]	f [Hz]
25k	-12.86±10.05	3.84	0.91±79.72	1.92
49k	-10.66±7.72	3.79	1.67±74.19	1.90
ref.	-14.58±12.44	3.86	1.23±80.6	1.93

Table 5: FSI2 results (forces)

size	drag [N m ⁻¹]	f [Hz]	lift [N m ⁻¹]	f [Hz]
25k	209.40±27.79	3.84	0.28±269.73	1.92
49k	212.51±22.85	3.79	-1.81±278.91	1.90
ref.	208.83±73.75	3.86	0.88±234.2	1.93

The coupled simulation converged with an average number of 3.8 iterations. The agreement in terms of tip displacement is good, in particular with the coarser mesh and 5 beam elements (Figure 7 shows the results). Some differences are present in the oscillating component of the forces.

4.4 FSI3

The last test case is characterized by a *mass ratio* $M = 1$ and an average *Reynolds number* $Re = 200$. This case has been widely studied and a review of results obtained with different approaches (monolithic or partitioned, with different solution strategies) can be found in [16].

The behavior of the structure in terms of tip displacement (mean value, amplitude and frequency) is shown in Table 6, while drag and lift on the whole structure are shown in Table 7.

The coupled simulation converged with an average number of 3.5 iterations (Figure 8 shows the results). As pointed out in [16], different solution approaches lead to differences of up to 50% for the drag and lift values, and up to 10% for the displacement values.

In our simulations, different discretizations lead to quite different solutions and the trade-off between the efficiency of a coarser mesh and the accuracy of a finer one is apparent. Besides, other simulation parameters have an impact on the results: e.g. the *structural damping* of the elastic beam changes the amplitude of the y component of the

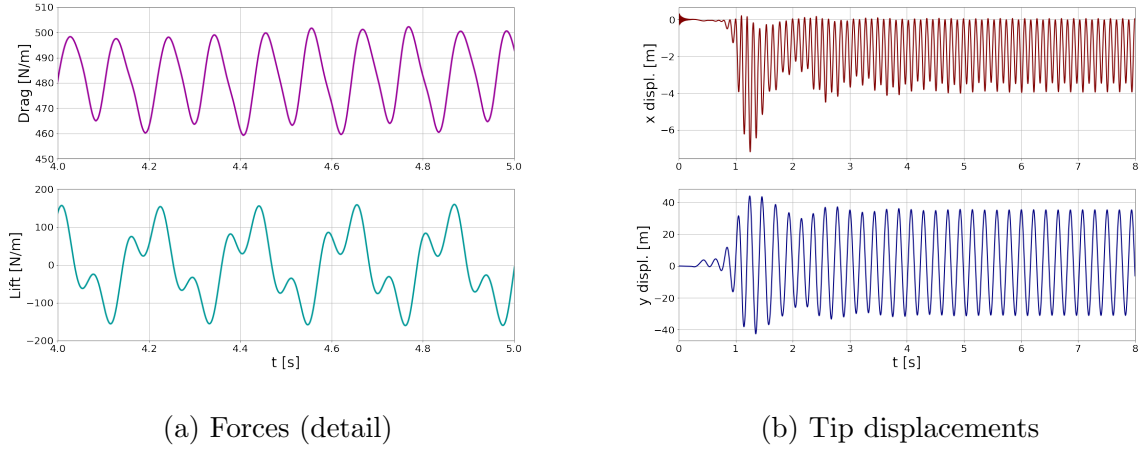


Figure 8: FSI3 Simulation: 4 beams - 49k cells

Table 6: FSI3 results (displacements)

size	N	u_x [mm]	f [Hz]	u_y [mm]	f [Hz]
25k	5	-3.76 ± 2.9	8.86	1.14 ± 46.92	4.43
49k	5	-1.91 ± 1.91	9.26	2.17 ± 33.78	4.63
25k	4	-3.51 ± 2.77	9.24	1.38 ± 45.9	4.59
49k	4	-1.83 ± 1.85	9.32	2.12 ± 33.06	4.66
ref.		-2.69 ± 2.53	10.9	1.48 ± 34.38	5.3

Table 7: FSI3 results (forces)

size	N	drag [N m^{-1}]	f [Hz]	lift [N m^{-1}]	f [Hz]
25k	5	515.54 ± 35.07	8.87	-1.28 ± 78.65	4.43
49k	5	481.24 ± 17.64	9.26	-0.48 ± 164.52	4.63
25k	4	502.62 ± 30.03	9.24	1.51 ± 97.31	4.59
49k	4	481.12 ± 19.07	9.32	-0.20 ± 157.64	4.66
ref.		457.3 ± 22.66	10.9	2.22 ± 149.78	5.3

tip displacement and the oscillation frequency. This last result appears to be lower than most of other studies in literature and might require a better tuning of the simulation of parameters.

5 CONCLUSIONS

The proposed adapter shows a good agreement with the considered benchmarks. Despite considering quite simple meshes, most results reported here look close to the reference values, showing that the current implementation proved to be robust with respect to strong interaction (high mass ratio). Thorough assessment in compressible regime (e.g. aeroelasticity) is underway.

Even though it must be thoroughly tested in realistic scenarios, the overall set-up proved to be flexible, widely configurable and tunable. In particular the ability to progressively load the structure at the beginning of the simulation turned out to be a very useful feature.

The adapter exploits the features provided by MBDyn for partitioned cosimulations and, via the common interfacier preCICE, it can connect MBDyn to virtually any solver, to perform FSI (fluid-solid interaction) and possibly hybrid multi-body full finite element simulations. It still requires some minor improvements, e.g. to use *nearest-projection* mappings in preCICE.

The code is independent of the MBDyn source code, which makes it easily extensible and maintainable.

References

- [1] Olivier A Bauchau et al. “Validation of flexible multibody dynamics beam formulations using benchmark problems”. In: *Multibody system dynamics* 37.1 (2016), pp. 29–48.
- [2] David Blom et al. “A Review on Fast Quasi-Newton and Accelerated Fixed-Point Iterations for Partitioned Fluid–Structure Interaction Simulation”. In: *Advances in Computational Fluid-Structure Interaction and Flow Simulation*. Springer, 2016, pp. 257–269.
- [3] Hans-Joachim Bungartz et al. “preCICE—a fully parallel library for multi-physics surface coupling”. In: *Computers & Fluids* 141 (2016), pp. 250–258.
- [4] Alessandro Cocco et al. “Simulation of Tiltrotor Maneuvers by a Coupled Multibody-Mid Fidelity Aerodynamic Solver”. In: *46th European Rotorcraft Forum (ERF 2020)*. 2020, pp. 1–8.
- [5] J Degroote et al. “An interface quasi-Newton algorithm for partitioned simulation of fluid-structure interaction”. In: *International Workshop on Fluid-Structure Interaction. Theory, Numerics and Applications*. kassel university press GmbH. 2009, p. 55.
- [6] Joris Degroote, Klaus-Jürgen Bathe, and Jan Vierendeels. “Performance of a new partitioned procedure versus a monolithic procedure in fluid–structure interaction”. In: *Computers & Structures* 87.11-12 (2009), pp. 793–801.
- [7] Joris Degroote et al. “Stability of a coupling technique for partitioned solvers in FSI applications”. In: *Computers & Structures* 86.23-24 (2008), pp. 2224–2234.

- [8] Gian Luca Ghiringhelli, Pierangelo Masarati, and Paolo Mantegazza. “Multibody implementation of finite volume C^0 beams”. In: *AIAA journal* 38.1 (2000), pp. 131–138.
- [9] Rob Haelterman et al. “Improving the performance of the partitioned QN-ILS procedure for fluid–structure interaction problems: Filtering”. In: *Computers & Structures* 171 (2016), pp. 9–17.
- [10] Pierangelo Masarati, Marco Morandini, and Paolo Mantegazza. “An efficient formulation for general-purpose multibody/multiphysics analysis”. In: *Journal of Computational and Nonlinear Dynamics* 9.4 (2014).
- [11] Miriam Mehl et al. “Parallel coupling numerics for partitioned fluid–structure interaction simulations”. In: *Computers & Mathematics with Applications* 71.4 (2016), pp. 869–891.
- [12] Giuseppe Quaranta, Pierangelo Masarati, and Paolo Mantegazza. “A conservative mesh-free approach for fluid-structure interface problems”. In: *International Conference for Coupled Problems in Science and Engineering, Greece*. 2005.
- [13] Thomas Richter and Thomas Wick. “On time discretizations of fluid-structure interactions”. In: *Multiple Shooting and Time Domain Decomposition Methods*. Springer, 2015, pp. 377–400.
- [14] Stefan Turek and Jaroslav Hron. “Proposal for numerical benchmarking of fluid-structure interaction between an elastic object and laminar incompressible flow”. In: *Fluid-structure interaction*. Springer, 2006, pp. 371–385.
- [15] Stefan Turek, Jaroslav Hron, and Mudassar Razzaq. “Numerical benchmarking of fluid-structure interaction between elastic object and laminar incompressible flow”. In: *Universitätsbibliothek Dortmund* (2010).
- [16] Stefan Turek et al. “Numerical Benchmarking of Fluid-Structure Interaction: A Comparison of Different Discretization and Solution Approaches”. In: vol. 73. Sept. 2010, pp. 413–424. ISBN: 978-3-642-14205-5. DOI: 10.1007/978-3-642-14206-2_15.
- [17] Stefan Turek et al. “Numerical Simulation and Benchmarking of a Monolithic Multi-grid Solver for Fluid-Structure Interaction Problems with Application to Hemodynamics”. In: vol. 73. Sept. 2010, pp. 193–220. ISBN: 978-3-642-14205-5. DOI: 10.1007/978-3-642-14206-2_8.
- [18] Benjamin Uekermann et al. “Official preCICE adapters for standard open-source solvers”. In: *Proceedings of the 7th GACM Colloquium on Computational Mechanics for Young Scientists from Academia*. 2017.